Host–Guest Systems

International Edition: DOI: 10.1002/anie.201502960
German Edition: DOI: 10.1002/ange.201502960

Halogen Bonding Molecular Capsules**

*Oliver Dumele, Nils Trapp, and François Diederich**

Dedicated to Prof. Albert Eschenmoser at the occasion of his 90th birthday

Abstract: *Molecular capsules based solely on the interaction of halogen bonding (XB) are presented along with their host–guest binding properties in solution. The first example of a well-defined four-point XB supramolecular system is realized by decorating resorcin[4]arene cavitands with polarized halogen atoms for dimerization with tetra(4-pyridyl) resorcin[4]arene cavitands. NMR binding data for the F, Cl, Br, and I cavitands as the XB donor show association constants (K_a) of up to 5370 M^{-1} ($\Delta G_{283\,K} = -4.85$ kcal mol^{-1}, for I), even in XB-competitive solvent, such as deuterated benzene/acetone/methanol (70:30:1) at 283 K, where comparable monodentate model systems show no association. The XB capsular geometry is evidenced by two-dimensional HOESY NMR, and the thermodynamic profile shows that capsule formation is enthalpically driven. Either 1,4-dioxane or 1,4-dithiane are encapsulated within each of the two separate cavities within the XB capsule, with of up to $K_a = 9.0\ 10^8\ M^{-2}$ ($\Delta G_{283\,K} = -11.6$ kcal mol^{-1}).*

The first covalently bonded molecular containers, carcerands, were reported by Cram et al. in 1985 and complexation and reactivity within their unique inner phase were investigated.[1] In the following years, various types of noncovalent intermolecular interactions were employed to construct supramolecular containers.[2–4] The first supramolecular, tennis-ball-shaped capsule capable of guest encapsulation was assembled by Rebek and co-workers by taking advantage of an elegantly designed hydrogen-bonding network between two hemispheres.[2] This work was followed by the introduction of metal–ligand coordination cages by Fujita et al.,[3] ionic capsular assembly by Verboom and co-workers,[4] and a hybrid of the aforementioned.[5] Herein we report the first molecular capsules assembled purely based on fourfold halogen bonding (XB), as well as their guest encapsulation properties in solution (Figure 1).[6]

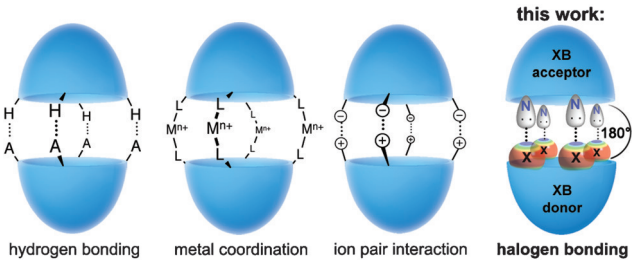

Figure 1. Various supramolecular capsules based on different interactions, and the first halogen bonding (XB) molecular capsule.

The importance of weak noncovalent interactions, such as XB, is emerging in many fields of chemistry. XB has received attention through its frequent application in crystal engineering.[7] More recently, it was implemented in complex supramolecular architectures[8] such as rotaxanes,[8a] catenanes,[8b] chiral macrocyclic hosts,[8d] and fluorescent anion sensors.[8e] In medicinal chemistry, XB has become an important tool in the development of more active and selective ligands.[9] Model system studies in solution[9e,10] revealed that the establishment of a single XB is largely enthalpy driven, but this gain in enthalpy is mostly compensated by a large unfavorable entropic term. The latter arises from the rigorous geometric prerequisites for efficient XB, that is, C–X···A angles (A: XB acceptor atom) close to 180° and the required sub-van der Waals contact between the XB donor and acceptor.[11] We hoped that the entropy loss would be reduced in the fourfold XB interactions established in our capsular assembly of highly preorganized components, as is well established for other multidentate bonding systems.[2e,8e,10c,12]

We selected top-rim-functionalized resorcin[4]arene cavitands as a concave, fourfold symmetric platform to generate the two hemispheres of the XB capsule. Benzimidazole walls on the cavitand scaffold, as introduced by Rebek and co-workers,[13] allowed the installation of various substituents at the upwards-pointing (2-)position leading to vertical exit vectors for XB donor and acceptor motifs (Scheme 1). Additionally, these extended benzimidazole cavitands are conformationally highly preorganized as they exhibit a persistent vase conformation. That conformation is particularly the case in the presence of alcohols, which bridge and rigidify the benzimidazole walls through a cyclic network of hydrogen bonds, as shown by Rebek and co-workers.[13]

2,3,5,6-Tetrafluoro-4-halophenyl and pyridyl moieties were chosen for the donor and acceptor motifs, respectively. C–X bond polarization through electron-withdrawing groups on the phenyl ring of halophenyl XB donors is commonly applied to the construction of XB architectures.[7b,8c,10b,c]

[*] O. Dumele, Dr. N. Trapp, Prof. Dr. F. Diederich
Laboratorium für Organische Chemie, ETH Zurich
Vladimir-Prelog-Weg 3, CH-8093 Zurich (Switzerland)
E-mail: diederich@org.chem.ethz.ch

[**] O.D. was supported by a Kekulé fellowship (Fonds der Chemischen Industrie) and the Studienstiftung des Deutschen Volkes. We are grateful for support by the ETH research council. We thank René Arnold and Dr. Marc-Olivier Ebert for recording 2D NMR spectra, Michael Solar for measuring X-ray crystal structures, Prof. Dr. Carlo Thilgen for help with the nomenclature, and Dr. Tristan Reekie and Dr. Bruno Bernet (all ETHZ) for valuable comments on the manuscript.

Supporting information for this article is available on the WWW under http://dx.doi.org/10.1002/anie.201502960.

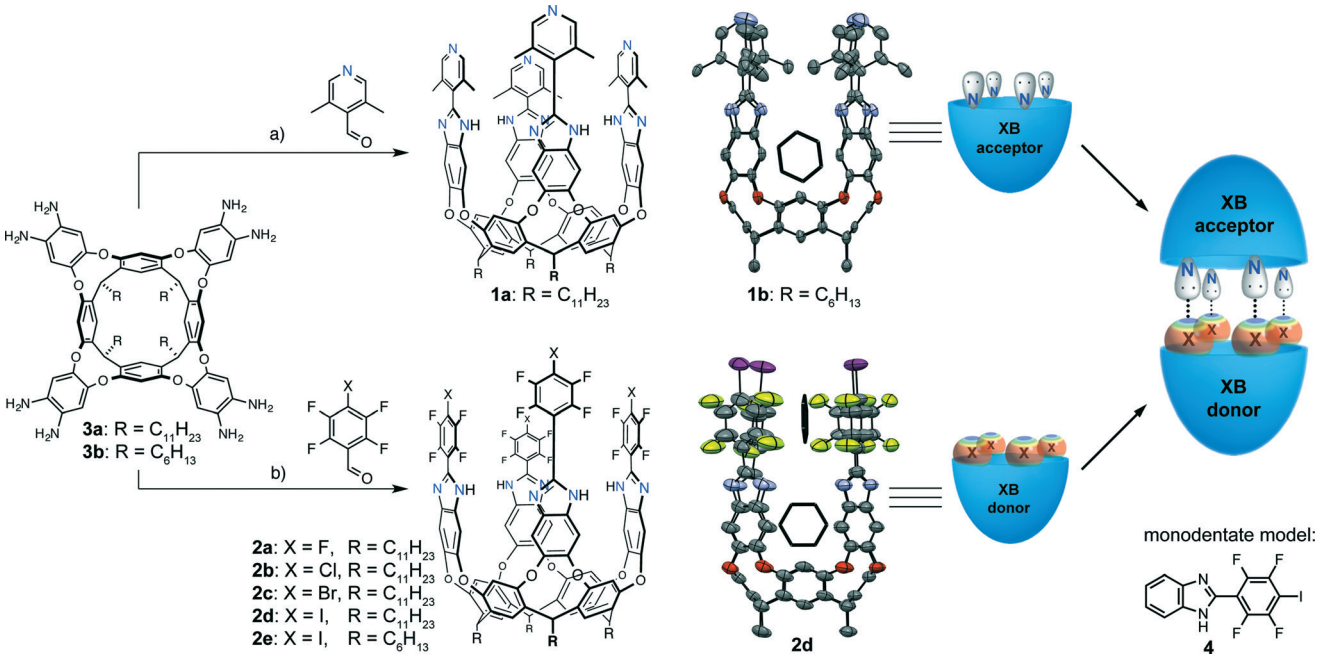

Scheme 1. Left: Synthesis of the cavitands **1a,b** and **2a–e** which were subjected to investigation of XB-mediated capsule formation. Reagents and conditions: a) 55 °C, 140 min, then $FeCl_3{\cdot}6H_2O$ (cat.), 70 °C, 17 h; b) 25 °C, 2–18 h, then $FeCl_3{\cdot}6H_2O$ (cat.), 25–55 °C, 20 h (X = F, Cl, Br, I). Right: X-ray crystal structures of **1b** (R = C_6H_{13}) and **2d** (R = $C_{11}H_{23}$).[21] Solvent molecules, R-alkyl groups, and hydrogen atoms are omitted for clarity. Thermal ellipsoids are shown at the 50% probability level at 100 K, and benzene guest molecules are drawn as stick model (see Section S6 in the Supporting Information). Bottom right: The XB donor **4** serves as monodentate comparison probe.

Pyridine, however, is known to be the weakest XB acceptor among hitherto quantified nitrogen Lewis bases,[10a,d] but nevertheless, we expected amplified association for such motifs to form the targeted capsules because of the cooperativity effect of tetradentate XB.

The synthesis of the XB acceptor hemispheres **1a**,**b** and XB donor hemispheres **2a–e** was based on the catalytic oxidative benzimidazole formation between the octamine cavitands **3a**,**b** and benzaldehyde derivatives as developed by Singh et al.,[14] and later applied to the construction of extended cavitands by Rebek and co-workers (Scheme 1, left).[13b]

Undecyl alkyl legs (**1a**, **2a–d**) were installed at the lower rim of the cavitands for enhanced solubility, whereas hexyl legs (**1b**, **2e**) were the choice for obtaining single-crystals suitable for X-ray crystallography. Thereby, the design criteria of vertical exit vectors of the XB motifs could be confirmed by the X-ray crystal structures obtained for **1b**, **2e**, and even the undecyl-legged cavitand **2d** (Scheme 1, right). These crystal structures also revealed the inclusion of two orthogonally edge-to-edge stacked benzene molecules in the tetraiodo cavitands **2d**,**e** and one benzene molecule deep inside the tetralutidine cavitand **1b**, entrapped by the four inwards converging methyl groups of the lutidyl moieties.

Association constants (K_a) for the complexation of **1a**···**2a–d** were determined by titrations monitored by ^{19}F NMR spectroscopy in an optimized solvent system of deuterated benzene/acetone/methanol (70:30:1), which fully solubilizes all components involved in this study. A minimum amount of alcohol solvent is crucial for the solubility and for bridging the benzimidazole wall flaps by hydrogen bonding, as was observed in all X-ray structures (see Figure 2E and Sections S3.1 and S6 in the Supporting Information).[13b] The temperature for all binding studies was adjusted to 283 K to minimize the unfavored $T\Delta S_{XB}$ term upon complexation and allow the quantification of even very weak XB motifs. When applying these conditions, fast exchange rates relative to the NMR time scale of the investigated XB capsule formation were observed in all cases.

We firstly investigated the tetrapyridine version **S6** as an analogue of **1a** in XB capsule association studies (see Figures S14 and S15 in the Supporting Information). However, upon formation of the (most likely) capsular assembly **S6**···**2d**, a precipitate formed (298 K). Hence, the eight additional methyl groups in **1a** compared to **S6** seem to be an essential structural modification for successful XB quantification in solution. Complexation experiments with **1a** ensured homogenous titration conditions at all times, and it was therefore constantly employed as a XB acceptor hemisphere, whereas the XB donor hemisphere was systematically varied by altering only the upper halogen atoms within the full range of F, Cl, Br, and I.

Binding isotherms generated from the ^{19}F NMR data show the greatest change in chemical shifts for **1a**···**2d** [$\Delta\delta_{sat}$(**2d**, F_{ortho}) = 1.26 ppm] as compared to all other XB donor cavitands (**2a–c**) subjected to titrations with **1a** [$\Delta\delta_{sat}$(**2a–c**, F_{ortho}) = 0.07 ppm; Figures 2A–C and Table 1]. The free enthalpy of binding, ΔG, for the XB capsule formation of **1a**···**2d** is −4.83 kcal mol^{-1} (association constant K_a = 5370 M^{-1}) in the aforementioned solvent system at 283 K (Table 1; for all titration data along with detailed analysis see Section S3).

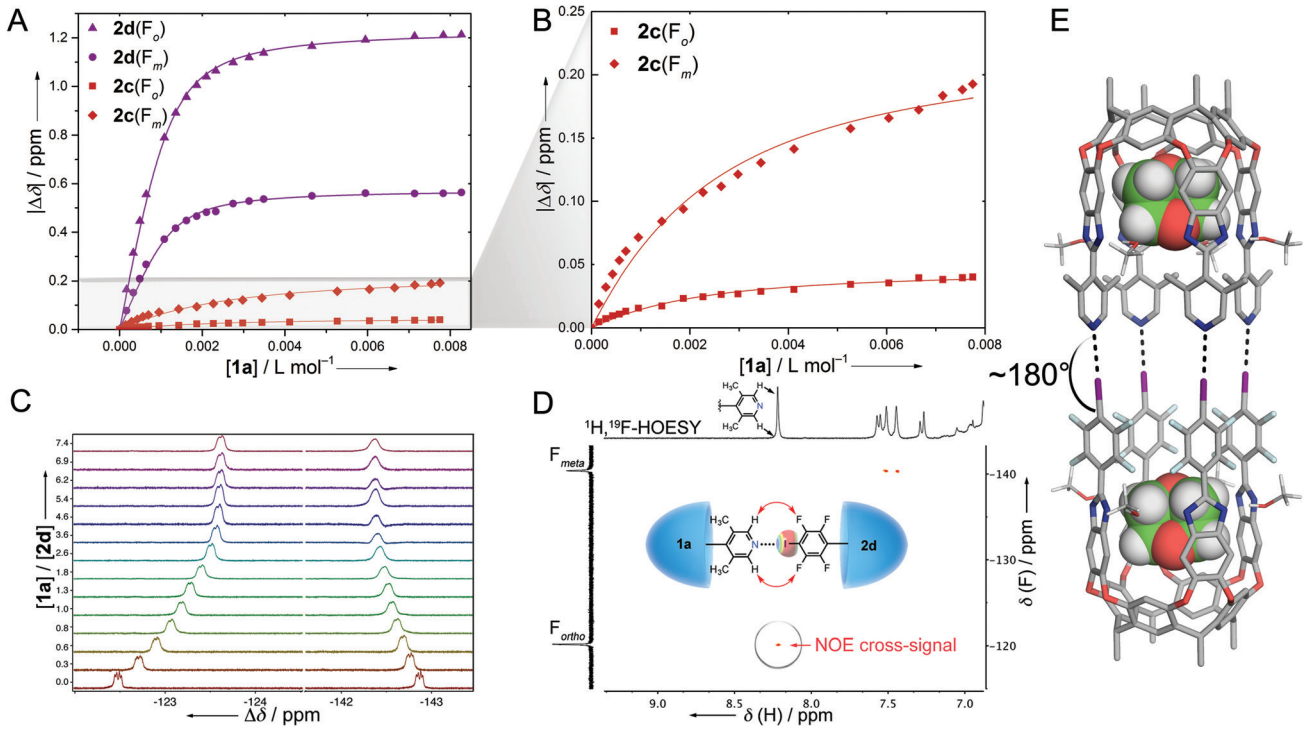

Figure 2. A) ^{19}F NMR binding titrations of tetrabromo (**2c**) and tetraiodo (**2d**) cavitands with **1a**. ^{19}F NMR signals for F_o and F_m atoms, relative to the halogen substituent in **2c**,**d**, were observed. Curve-fitting to 1:1 isotherms is shown as a solid line. For titrations of **2a**,**b** with **1a**, no meaningful curve-fitting was possible. B) Zoomed-in view on the grey inset box of A: ^{19}F NMR binding titrations of **2c** with **1a**. C) Titration progress observed by ^{19}F NMR spectroscopy of **2d** (addition of **1a**). D) ^{1}H,^{19}F HOESY NMR spectrum of **1a**···**2d** in [D_{12}]mesitylene (+2% 3,5-dimethylbenzyl alcohol) at 283 K, which shows a cross-signal for the intermolecular through-space H···F coupling between **1a** and **2d** with two 1,4-dithianes encapsulated as guest molecules (not shown). Conditions of titrations for figures (A)–(C): $C_6D_6/(CD_3)_2CO/CD_3OD$ (70:30:1) at 283 K, c_0(**2c**,**d**) ≈ 1.5 mM. E) Calculated model for XB capsule **1a**···**2d** with two 1,4-dioxane guests and four MeOH bridging units to stabilize intramolecular hydrogen bonding between imidazole walls (nearly optimized at the DFT:B3LYP/cc-pVDZ-LANL2DZ level of theory; see Section S7 in the Supporting Information).

Table 1: Association constants (K_a) and derived binding free enthalpies (ΔG) of the XB donors **2a–d** with the XB acceptor **1a**, and thermodynamic profile of the XB capsule **1a**···**2d**.

Complex	X	$K_{a,283\,K}$[a] [M^{-1}]	$\Delta G_{283\,K}$[b] [kcal mol^{-1}]	$\Delta\delta_{sat}(F_{ortho}/F_{meta})$ [ppm]
1a···**2d**	I	5370	−4.83	1.26/0.59
1a···**2c**	Br	602	−3.60	0.05/0.23
1a···**2b**	Cl	–[c]	–	0.07/0.02
1a···**2a**	F	–[c]	–	0.07/0.03[d]
4···3,5-lutidine	I	< 1	–	–[c]
		$\Delta G_{283\,K}$[e] [kcal mol^{-1}]	ΔH[e] [kcal mol^{-1}]	$T\Delta S$[e] [kcal mol^{-1}]
1a···**2d**	I	−4.87	−12.61	−7.75 (283 K)

[a] In $C_6D_6/(CD_3)_2CO/CD_3OD$ (70:30:1) at 283 K. Determined by curve-fitting of ^{19}F NMR titration data to 1:1 binding isotherms. Error estimated to be ca. 20%. [b] Calculated from K_a. [c] No meaningful curve-fitting of the titration isotherms was possible. [d] $\Delta\delta_{sat}(F_{ipso}) = 0.13$ ppm. [e] Determined by van't Hoff analysis of VT-NMR binding titrations (see Section S3.4).

The binding mode of the capsular geometry was confirmed by ^{1}H,^{19}F HOESY NMR methods[15] with a cross-signal for the intermolecular through-space coupling of the H-C(2,6) protons of the lutidyl moieties in **1a** with only the F_{ortho} atoms (relative to to the iodo substituent) in **2d** in two independent experiments (Figure 2D and Section S3.7). The 1:1 stoichiometry of the capsular assembly was confirmed by continuous variation methods (Job plot analysis), and MALDI-MS showed signals corresponding to the molecular ion of the 1:1 XB complex (see Sections S3.5 and S3.6).[16] A DFT model of **1a**···**2d** supports the complementary geometry of the cavitands with XB angles close to 180° (Figure 2E). Methods to obtain a single-crystal suitable for X-ray crystallography of **1b**···**2e** are currently being developed in our laboratory.

By subjecting **2c** to binding titrations with **1a**, it was even possible to determine XB association constants for organobromines for the first time. This quantification experiment is remarkable considering the weak acceptor character of the pyridyl moieties in **1a** and the competitive solvent system. Although the absolute changes in chemical shift of both fluorine atoms *ortho* and *meta* to the bromo substituent in **2c** were small compared to those in **2d**, nonlinear curve-fittings to the 1:1 isotherms resulted in reliable parameters for K_a and $\Delta\delta_{sat}$ (Figures 2A,B). The association constant for **2c** with **1a** is $K_a = 602\,M^{-1}$, a magnitude lower than observed for the complexation of the **2d**, and is thus reflected in a $\Delta\Delta G_{2c\text{-}2d}$ increment of 1.23 kcal mol^{-1} at 283 K. Hence, the difference for establishing XB with iodine compared to bromine is

$\Delta\Delta G_{Br\rightarrow I} = -0.31$ kcal mol^{-1} per XB formed in the given solvent conditions.

Titrations of Cl (**2b**) and F (**2a**) derivatives with **1a** resulted in minor changes of the ^{19}F NMR chemical shifts, and no meaningful curve fitting to 1:1 binding isotherms was obtained for any of the observed ^{19}F signals (fitting errors are within the range or greater than the resulting parameter values for K_a and $\Delta\delta_{sat}$; see Figures S7–11 in the Supporting Information).

For comparison of the four-point XB capsule to a monodentate XB assembly of the same binding motif, the association constant for **4**···3,5-lutidine (Scheme 1, right) was determined and the binding was found to be too weak to allow a precise analysis by NMR binding titration ($K_a < 1$ M^{-1}, aforementioned solvent system, 283 K, see Figures S12 and S13 in the Supporting Information). Along these lines, earlier solution studies on monodentate perfluoroiodoalkanes with pyridine as the XB acceptor showed that not even in apolar solvents (benzene, CCl_4, $CDCl_3$) significant association was observed ($K_a = 1$, 0.8, and < 0.5 M^{-1}, respectively for the listed solvents).[10a]

The substantial amplification of XB association in our multidentate XB capsules is clearly caused by intrinsically decreasing the unfavorable $T\Delta S$ term through a multidentate assembly, as confirmed by van't Hoff analysis of the complexation of **1a**···**2d** (see Section S3.4). The formation of the XB capsule is enthalpy-driven by $\Delta H = -12.6$ kcal mol^{-1} and entropically disfavored by $T\Delta S = -7.8$ kcal mol^{-1} at 283 K. In a simple picture, the complexation entropy is already compensated upon the formation of three halogen bonds, and the fourth XB can harvest the enthalpic gain without much additional loss in entropy. Upon formation of three XBs, the fourth halogen atom is restricted to undergo XB in such capsular assemblies.

Host–guest binding studies of **1a**···**2d** with 1,4-dioxane and 1,4-dithiane reveal the shape, volume, and guest affinity of the inner space of the XB capsule.[2b,17] To conduct these studies, we developed a noncompetitive solvent system consisting of [D$_{12}$]mesitylene with 2% of 3,5-dimethylbenzyl alcohol, an alcohol to stabilize the cavitands' conformations by circular hydrogen bonding to the imidazole moieties without occupying the cavity, while providing full solubility (see Section S4.1).

In a first step, we investigated binding to only the single cavitands **1a** and **2d** by employing 1,4-dioxane and 1,4-dithiane as guests. The encapsulated guests show slow exchange rates relative to the NMR time scale (aforementioned solvent system, 283 K), and their chemical shifts appear in the negative ppm region, which is typical for top-closed cavitands and molecular capsules with aromatic scaffolds.[13b,18] Binding constants (K_a) were determined from the integration ratio between the signals of free and the bound guest. In case the ^{1}H NMR resonance of the free guest overlapped with other signals of the sample, hexakis-[(trimethylsilyl)ethynyl]benzene[19] (**S14**) was employed as particularly bulky, yet symmetrical internal standard, to determine the concentration of the free guest (see Section S4.1). The free enthalpy of binding of 1,4-dioxane to **1a** and **2d** are -3.8 and -3.3 kcal mol^{-1}, respectively, whereas

Table 2: Host–guest binding data for 1,4-dioxane and 1,2-dithiane binding to **1a**, **2d**, and **1a**···**2d**.

Guest	Host	$K_{a,283\,K}$[a]	$\Delta G_{283\,K}$[b] [kcal mol^{-1}]
1,4-dioxane	**1a**	8.9×10^2 M^{-1}	−3.8
	2d	3.6×10^2 M^{-1}	−3.3
	1a···**2d**	5.8×10^5 M^{-2}	−7.5
1,4-dithiane	**1a**	1.0×10^4 M^{-1}	−5.2
	2d	3.4×10^4 M^{-1}	−5.9
	1a···**2d**	9.0×10^8 M^{-2}	−11.6

[a] K_a value determined by ^{1}H NMR integration ratios of bound and free guest in [D$_{12}$]mesitylene (+2% 3,5-dimethylbenzyl alcohol) at 283 K; errors in K_a are estimated to be ca. 20%. [b] Calculated from $K_{a,\,283\,K}$.

1,4-dithiane binds with $\Delta G_{283\,K}$ of -5.2 and -5.9 kcal mol^{-1}, respectively (Table 2). The cavity volume of **1a** is smaller than that of **2d**, and 1,4-dioxane shows higher affinities to **1a**, whereas the larger 1,4-dithiane guest fits better in the cavity of **2d** (for cavity volumes see Section S4.4 in the Supporting Information).

In the quantification of guest binding to the XB capsule **1a**···**2d**, slow exchange of the guests relative to the NMR time scale was maintained, while the exchange rate for XB capsule formation remained fast. The presence of the capsular geometry during guest binding experiments was confirmed by ^{1}H,^{19}F HOESY NMR spectroscopy (see Section S3.7). Significant changes in the ^{1}H NMR chemical shifts of the guest protons inside the capsule **1a**···**2d**, as compared to the complexes of the single cavitands **1a** and **2d**, were observed (Figure 3). The XB capsule **1a**···**2d** does not feature a single elongated cavity but two separated compartments in the two associating cavitands. The four lutidine methyl groups converge into the cavity, thus providing a steric barrier for communication between the two hemispheres in the capsule (X-ray in Scheme 1). The 1,4-dioxane or 1,4-dithiane guests fill both compartments in the capsule, thus resulting in a 1:2 host/guest stoichiometry for the capsular complexes of the

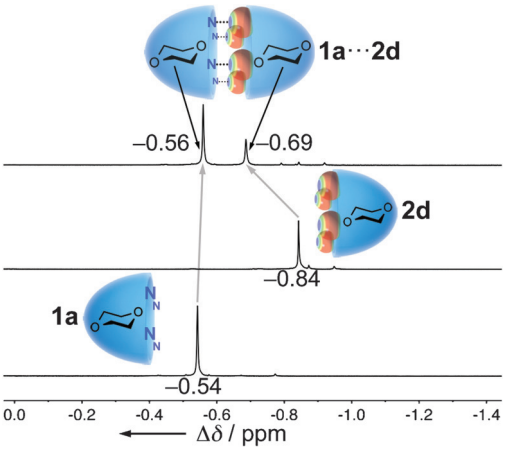

Figure 3. ^{1}H NMR spectra of 1,4-dioxane encapsulated within **1a**···**2d**, **2d**, and **1a**, in [D$_{12}$]mesitylene (+2% 3,5-dimethylbenzyl alcohol) at 283 K. Locations of guests were determined by ^{1}H,^{19}F HOESY NMR spectra (see Section S4.3). ^{1}H NMR chemical shifts of the corresponding signals are given in ppm.

type [(guest ⊂ **1a**)···(guest ⊂ **2d**)]. For **1a**···**2d** as the host, the position of the guests, located either in the **1a** or the **2d** hemisphere, was determined by assigning each ^{1}H NMR signal with ^{1}H,^{19}F HOESY NMR techniques (Figure 3). In such experiments, the ^{1}H NMR resonances of the guest show cross-signals of strong intensity with the F_{meta} atoms and cross-signals of weak intensity with the F_{ortho} atoms of the **2d** hemisphere (see Section S4.3).

The most stable association was observed for the complex (1,4-dithiane)$_2$ ⊂ **1a**···**2d** ($\Delta G = -11.6$ kcal mol^{-1}). The association of 1,4-dithiane to all three molecular hosts, **1a**, **2d**, and **1a**···**2d**, is stronger than that of 1,4-dioxane (Table 2), and is attributed to dispersive S···π interactions and possibly S···N interactions.[20] Gains in ΔG of -0.4 kcal mol^{-1} for 1,4-dioxane and -0.5 kcal mol^{-1} for 1,4-dithiane binding in the XB capsule are observed when compared to the binding within the single cavitands. We attribute this insignificant enhancement of guest affinities in the XB capsule to only a small change in the geometry and electronic environment of the inner cavities which remain nearly unchanged upon formation of the XB capsule.

In summary, we present the first example for the formation of supramolecular XB capsules in solution by installing tetrafluorohalophenyl motifs as XB donors and lutidyl moieties as XB acceptors on resorcin[4]arene cavitand scaffolds. Multidentate four-point XB was realized for X = I and Br by fulfilling the 180° angle as a binding criterion simultaneously for all four XBs formed in the assembly. No structured association was found for the F and Cl derivatives (**2a** and **2b**). The strongest XB capsule was formed with the tetraiodo cavitand **2d** complexed with tetralutidine cavitand **1a** in the competitive solvent C_6D_6/$(CD_3)_2CO$/CD_3OD (70:30:1) at 283 K. Van't Hoff analysis revealed the thermodynamic profile of the XB capsule **1a**···**2d** to be largely enthalpy driven, from which we conclude that decreasing the entropic term of XB by multidentate binding is the key to self-assembly of even weak binding partners such as the pyridine derivative **1a**. We further demonstrated guest binding to the XB capsule **1a**···**2d**, which features two separated compartments. Binding free enthalpies down to -11.6 kcal mol^{-1} were measured for the 1:2 complex of 1,4-dithiane in **1a**···**2d** at 283 K in [D_{12}]mesitylene (+2% 3,5-dimethylbenzyl alcohol). With this example of a highly defined noncovalent structure assembled solely by XB, we clearly expect further applications of halogen bonding in future supramolecular architectures.

Keywords: halogen bonding · host-guest systems · self-assembly · supramolecular chemistry · X-ray diffraction

How to cite: *Angew. Chem. Int. Ed.* **2015**, *54*, 12339–12344
Angew. Chem. **2015**, *127*, 12516–12521

[1] a) D. J. Cram, S. Karbach, Y. H. Kim, L. Baczynskyj, G. W. Kallemeyn, *J. Am. Chem. Soc.* **1985**, *107*, 2575–2576; b) D. J. Cram, S. Karbach, Y. H. Kim, L. Baczynskyj, K. Marti, R. M. Sampson, G. W. Kalleymeyn, *J. Am. Chem. Soc.* **1988**, *110*, 2554–2560; c) D. J. Cram, J. M. Cram, *Container Molecules and Their Guests*, The Royal Society of Chemistry, Cambridge, **1994**; d) A. Jasat, J. C. Sherman, *Chem. Rev.* **1999**, *99*, 931–968; e) R. Warmuth, J. Yoon, *Acc. Chem. Res.* **2001**, *34*, 95–105.

[2] a) R. Wyler, J. de Mendoza, J. Rebek, Jr., *Angew. Chem. Int. Ed. Engl.* **1993**, *32*, 1699–1701; *Angew. Chem.* **1993**, *105*, 1820–1821; b) F. Hof, S. L. Craig, C. Nuckolls, J. Rebek, Jr., *Angew. Chem. Int. Ed.* **2002**, *41*, 1488–1508; *Angew. Chem.* **2002**, *114*, 1556–1578; for selected work by others: c) O. Mogck, V. Böhmer, W. Vogt, *Tetrahedron* **1996**, *52*, 8489–8496; d) V. Böhmer, M. O. Vysotsky, *Aust. J. Chem.* **2001**, *54*, 671–677; e) L. J. Prins, D. N. Reinhoudt, P. Timmerman, *Angew. Chem. Int. Ed.* **2001**, *40*, 2382–2426; *Angew. Chem.* **2001**, *113*, 2446–2492.

[3] a) M. Fujita, S. Nagao, K. Ogura, *J. Am. Chem. Soc.* **1995**, *117*, 1649–1650; b) M. Fujita, *Chem. Soc. Rev.* **1998**, *27*, 417–425; for selected work by others: c) P. Jacopozzi, E. Dalcanale, *Angew. Chem. Int. Ed. Engl.* **1997**, *36*, 613–615; *Angew. Chem.* **1997**, *109*, 665–667; d) D. L. Caulder, K. N. Raymond, *J. Chem. Soc. Dalton Trans.* **1999**, 1185–1200; e) S. R. Seidel, P. J. Stang, *Acc. Chem. Res.* **2002**, *35*, 972–983; f) M. M. J. Smulders, I. A. Riddell, C. Browne, J. R. Nitschke, *Chem. Soc. Rev.* **2013**, *42*, 1728–1754.

[4] G. V. Oshovsky, D. N. Reinhoudt, W. Verboom, *J. Am. Chem. Soc.* **2006**, *128*, 5270–5278.

[5] M. Yamanaka, N. Toyoda, K. Kobayashi, *J. Am. Chem. Soc.* **2009**, *131*, 9880–9881.

[6] A model for the X-ray structure of a pseudocapsular assembly consisting of a tetra-(3-pyridyl) cavitand and a flexible iodinated calix[4]arene showed partly the XB dimer in the solid state besides other geometries (crystallographic *R*1-value = 21.4%): a) C. B. Aakeröy, A. Rajbanshi, P. Metrangolo, G. Resnati, M. F. Parisi, J. Desper, T. Pilati, *CrystEngComm* **2012**, *14*, 6366–6368; An XB donor with quadruple iodoethynyl motifs at the upper rim of a resorcin[4]arene cavitand has recently been reported, however, the desired formation of a dimeric capsular assembly with the pendant XB acceptor cavitand has not been observed: b) L. Turunen, N. K. Beyeh, F. Pan, A. Valkonen, K. Rissanen, *Chem. Commun.* **2014**, *50*, 15920–15923. For a recent X-ray structure of resorcinarene dimers linked by four ionic hydrogen-bonded chloride ions and two halogen-bonded I_2 molecules, see: c) N. K. Beyeh, F. Pan, K. Rissanen, *Angew. Chem. Int. Ed.* **2015**, DOI: 10.1002/anie.201501855; *Angew. Chem.* **2015**, DOI: 10.1002/ange.201501855.

[7] a) G. R. Desiraju, *Angew. Chem. Int. Ed. Engl.* **1995**, *34*, 2311–2327; *Angew. Chem.* **1995**, *107*, 2541–2558; b) P. Metrangolo, F. Meyer, T. Pilati, G. Resnati, G. Terraneo, *Angew. Chem. Int. Ed.* **2008**, *47*, 6114–6127; *Angew. Chem.* **2008**, *120*, 6206–6220; c) R. W. Troff, T. Mäkelä, F. Topić, A. Valkonen, K. Raatikainen, K. Rissanen, *Eur. J. Org. Chem.* **2013**, 1617–1637.

[8] a) N. L. Kilah, M. D. Wise, C. J. Serpell, A. L. Thompson, N. G. White, K. E. Christensen, P. D. Beer, *J. Am. Chem. Soc.* **2010**, *132*, 11893–11895; b) L. C. Gilday, T. Lang, A. Caballero, P. J. Costa, V. Félix, P. D. Beer, *Angew. Chem. Int. Ed.* **2013**, *52*, 4356–4360; *Angew. Chem.* **2013**, *125*, 4452–4456; c) T. M. Beale, M. G. Chudzinski, M. G. Sarwar, M. S. Taylor, *Chem. Soc. Rev.* **2013**, *42*, 1667–1680; d) S. Castro-Fernández, I. R. Lahoz, A. L. Llamas-Saiz, J. L. Alonso-Gómez, M.-M. Cid, A. Navarro-Vázquez, *Org. Lett.* **2014**, *16*, 1136–1139; e) B. R. Mullaney, A. L. Thompson, P. D. Beer, *Angew. Chem. Int. Ed.* **2014**, *53*, 11458–11462; *Angew. Chem.* **2014**, *126*, 11642–11646.

[9] a) P. Auffinger, F. A. Hays, E. Westhof, P. S. Ho, *Proc. Natl. Acad. Sci. USA* **2004**, *101*, 16789–16794; b) L. A. Hardegger, B. Kuhn, B. Spinnler, L. Anselm, R. Ecabert, M. Stihle, B. Gsell, R. Thoma, J. Diez, J. Benz, J.-M. Plancher, G. Hartmann, Y. Isshiki, K. Morikami, N. Shimma, W. Haap, D. W. Banner, F. Diederich, *ChemMedChem* **2011**, *6*, 2048–2054; c) L. A. Hardegger, B. Kuhn, B. Spinnler, L. Anselm, R. Ecabert, M. Stihle, B. Gsell, R. Thoma, J. Diez, J. Benz, J.-M. Plancher, G. Hartmann, D. W. Banner, W. Haap, F. Diederich, *Angew. Chem. Int. Ed.* **2011**, *50*,

314 – 318; *Angew. Chem.* **2011**, *123*, 329 – 334; d) R. Wilcken, M. O. Zimmermann, A. Lange, A. C. Joerger, F. M. Boeckler, *J. Med. Chem.* **2013**, *56*, 1363 – 1388; for a recent review on the impact for XB model systems on medicinal chemistry applications, see: e) E. Persch, O. Dumele, F. Diederich, *Angew. Chem. Int. Ed.* **2015**, *54*, 3290 – 3327; *Angew. Chem.* **2015**, *127*, 3341 – 3382.

[10] a) R. Cabot, C. A. Hunter, *Chem. Commun.* **2009**, 2005 – 2007; b) M. G. Sarwar, B. Dragisic, L. J. Salsberg, C. Gouliaras, M. S. Taylor, *J. Am. Chem. Soc.* **2010**, *132*, 1646 – 1653; c) S. H. Jungbauer, D. Bulfield, F. Kniep, C. W. Lehmann, E. Herdtweck, S. M. Huber, *J. Am. Chem. Soc.* **2014**, *136*, 16740 – 16743; d) O. Dumele, D. Wu, N. Trapp, N. Goroff, F. Diederich, *Org. Lett.* **2014**, *16*, 4722 – 4725.

[11] a) N. Ramasubbu, R. Parthasarathy, P. Murray-Rust, *J. Am. Chem. Soc.* **1986**, *108*, 4308 – 4314; b) J. P. M. Lommerse, A. J. Stone, R. Taylor, F. H. Allen, *J. Am. Chem. Soc.* **1996**, *118*, 3108 – 3116; c) K. E. Riley, K. M. Merz, Jr., *J. Phys. Chem. A* **2007**, *111*, 1688 – 1694; d) P. Politzer, J. S. Murray, T. Clark, *Phys. Chem. Chem. Phys.* **2010**, *12*, 7748 – 7757.

[12] L.-Y. You, S.-G. Chen, X. Zhao, Y. Liu, W.-X. Lan, Y. Zhang, H.-J. Lu, C.-Y. Cao, Z.-T. Li, *Angew. Chem. Int. Ed.* **2012**, *51*, 1657 – 1661; *Angew. Chem.* **2012**, *124*, 1689 – 1693.

[13] a) A. R. Far, A. Shivanyuk, J. Rebek, Jr., *J. Am. Chem. Soc.* **2002**, *124*, 2854 – 2855; b) E. Menozzi, H. Onagi, A. L. Rheingold, J. Rebek, Jr., *Eur. J. Org. Chem.* **2005**, 3633 – 3636.

[14] M. P. Singh, S. Sasmal, W. Lu, M. N. Chatterjee, *Synthesis* **2000**, 1380 – 1390.

[15] G. Ciancaleoni, R. Bertani, L. Rocchigiani, P. Sgarbossa, C. Zuccaccia, A. Macchioni, *Chem. Eur. J.* **2015**, *21*, 440 – 447.

[16] C. A. Schalley, R. K. Castellano, M. S. Brody, D. M. Rudkevich, G. Siuzdak, J. Rebek, Jr., *J. Am. Chem. Soc.* **1999**, *121*, 4568 – 4579.

[17] J. Rebek, Jr., *Acc. Chem. Res.* **2009**, *42*, 1660 – 1668.

[18] a) T. Heinz, D. M. Rudkevich, J. Rebek, Jr., *Nature* **1998**, *394*, 764 – 766; b) J. Hornung, D. Fankhauser, L. D. Shirtcliff, A. Praetorius, W. B. Schweizer, F. Diederich, *Chem. Eur. J.* **2011**, *17*, 12362 – 12371; c) I. Pochorovski, F. Diederich, *Acc. Chem. Res.* **2014**, *47*, 2096 – 2105.

[19] R. Diercks, J. C. Armstrong, R. Boese, K. P. C. Vollhardt, *Angew. Chem. Int. Ed. Engl.* **1986**, *25*, 268 – 269; *Angew. Chem.* **1986**, *98*, 270 – 271.

[20] B. R. Beno, K.-S. Yeung, M. D. Bartberger, L. D. Pennington, N. A. Meanwell, *J. Med. Chem.* **2015**, DOI: 10.1021/jm501853m.

[21] CCDC 1051314 (**1b**), 1051313 (**2d**), and 1051312 (**2e**) contain the supplementary crystallographic data for this paper. These data can be obtained free of charge from The Cambridge Crystallographic Data Centre via www.ccdc.cam.ac.uk/data_request/cif.

Received: March 31, 2015
Published online: May 26, 2015

